Received: 8 October 2019 | Revised: 17 February 2020 | Accepted: 26 March 2020

DOI: 10.1002/eqe.3278

WILEY

RESEARCH ARTICLE

The role of ground motion duration and pulse effects in the collapse of ductile systems

Maria Liapopoulou | **Miguel A. Bravo-Haro** | **Ahmed Y. Elghazouli**

Department of Civil and Environmental Engineering, Imperial College London, London, UK

Correspondence
A. Y. Elghazouli, Department of Civil and Environmental Engineering, Imperial College London, London, UK.
Email: a.elghazouli@imperial.ac.uk

Funding information
Onassis Foundation; Imperial College London

Summary

The seismic collapse capacity of ductile single-degree-of-freedom systems vulnerable to P-Δ effects is investigated by examining the respective influence of ground motion duration and acceleration pulses. The main objective is to provide simple relationships for predicting the duration-dependent collapse capacity of modern ductile systems. A novel procedure is proposed for modifying spectrally equivalent records, such that they are also equivalent in terms of pulses. The effect of duration is firstly assessed, without accounting for pulses, by assembling 101 pairs of long and short records with equivalent spectral response. The systems considered exhibit a trilinear backbone curve with an elastic, hardening and negative stiffness segment. The parameters investigated include the period, negative stiffness slope, ductility and strain hardening, for both bilinear and pinching hysteretic models. Incremental dynamic analysis is employed to determine collapse capacities and derive design collapse capacity spectra. It is shown that up to 60% reduction in collapse capacity can occur due to duration effects for flexible bilinear systems subjected to low levels of *P*-Δ. A comparative evaluation of intensity measures that account for spectral shape, duration or pulses, is also presented. The influence of pulses, quantified through incremental velocity, is then explicitly considered to modify the long records, such that their pulse distribution matches that of their short spectrally equivalent counterparts. The results show the need to account for pulse effects in order to achieve unbiased estimation of the role of duration in flexible ductile systems, as it can influence the duration-induced reduction in collapse capacity by more than 20%.

KEYWORDS

collapse capacity, ground motion duration, hysteretic behaviour, incremental velocity, intensity measures

1 | INTRODUCTION

Assessment of the seismic intensity that leads to structural collapse, typically defined as a disproportionate increase in deformation or the exceedance of a predefined deformation threshold,[1] is of fundamental importance in earthquake engineering. As a result, this has been the subject of various previous investigations, many of which have focused on the response of single-degree-of-freedom (SDOF) models, in which dynamic instability was represented through a decreasing branch in their backbone curve or through explicit inclusion of P-Δ effects. For example, Miranda and Akkar[2] studied the collapse capacity of simple structures, modelled as bilinear SDOF systems with a negative postyield stiffness, subjected to a suite of 72 ground motion records. Collapse capacity spectra were provided as a function of the SDOF period and the slope of the negative stiffness branch, and it was concluded that both lower levels of postyield stiffness, which is equivalent to lower levels of P-Δ, and higher values of structural period, increase the collapse capacity. More recently, similar conclusions were reached by Adam and Jäger,[3] who used bilinear, peak-oriented and pinching hysteretic models and an assembly of 44 far-field earthquake records. Instead of defining a negative branch in the backbone curve, gravity loads were explicitly applied to the SDOF model, causing rotation of the backbone due to P-Δ effects (i.e., geometric nonlinearity). Collapse capacity spectra were developed as a function of period, level of P-Δ, viscous damping and type of hysteresis. These spectra were later refined by Tsantaki et al.[4] The more general case of ductile systems with trilinear backbones and pinching hysteresis was examined by Vamvatsikos et al.[5] through deconstruction of the problem to determine the collapse capacity of a bilinear and an elastic-perfectly plastic system. Based on this simplification, an expression for the collapse capacity for different values of period, negative slope, ductility and strain hardening was derived. Ductile strength-degrading SDOFs with bilinear hysteresis were investigated by Han et al.[6] who developed equations for the median and dispersion of their collapse capacity, covering a wide range of system parameters (period, strain hardening ratio, negative slope, ductility and damping) and employing an ensemble of 240 ground motions.

None of the above described studies, however, considered the role of duration in the assessment of collapse capacity. Attempts to incorporate duration in this process have only recently been made, all indicating its importance. Foschaar et al.[7] compared collapse capacities of a steel concentrically braced frame subjected to the FEMA P695 record set[8] and sets of long-duration records, which were assembled based on different duration metrics. They reported a maximum of 60% reduction in collapse capacity of the long-duration set based on 5–95% significant duration[9] compared with the FEMA P695 set. Although the importance of considering the spectral shape for an accurate assessment of duration effects was pointed out, this was not addressed in the study. Raghunandan and Liel[10] employed the same definition of duration for the assessment of reinforced concrete frames subjected to long- and short-duration records and reported up to 56% reduction in median collapse capacity. The differences in spectral shape characteristics of the two sets were assumed to be captured by using spectral displacement as the intensity measure (IM). In another study, Raghunandan et al.[11] reported an average reduction of 36% in the median collapse capacity of ductile reinforced concrete frames and 12% for nonductile counterparts, when subjected to long-duration earthquakes. The effect of spectral shape was later explicitly considered by Chandramohan et al.[12] who assembled short and long records with equivalent response spectra to investigate the effect of duration on a steel moment resisting frame and a reinforced concrete bridge pier, recording 29% and 17% reduction in collapse capacity, respectively, when long records were used. Their results were based on 5–75% significant duration,[13] which was identified as the most appropriate duration metric. Bravo-Haro and Elghazouli[14] assembled 77 short and 77 spectrally equivalent long records, characterised by means of 5–75% significant duration, to assess four moment resisting frames and 50 equivalent SDOF (ESDOF) systems. They found up to 24% reduction in collapse capacity of the considered multi-degree-of-freedom (MDOF) systems due to longer duration, which increased to 40% for highly degrading ESDOF models. Using the same methodology, Bravo-Haro et al.[15] investigated duration effects for SDOF systems with bilinear backbone curves, reporting a maximum of about 50% reduction in their collapse capacity as a result of longer ground motion duration; design collapse capacity spectra, which capture the observed differences due to duration, were also provided.

Apart from the studies by Raghunandan and Liel[10] and Raghunandan et al.[11] the above-mentioned assessments employed spectral acceleration to quantify ground motion intensity. However, first-mode spectral acceleration was shown to be inefficient, which implies that it can result in relatively high dispersion of structural response (e.g., Kostinakis et al.[16] and Marafi et al.[17]). In order to attempt to overcome this shortcoming, other indexes have been proposed in the literature. Cordova et al.[18] suggested multiplying the spectral acceleration by a ratio of spectral ordinates that accounts for period lengthening due to nonlinearity and indicated that it can reduce the record-to-record variability. Luco and Cornell[19] suggested five IMs that account for inelasticity and higher mode effects by means of multiplying

the first-mode spectral acceleration by appropriate factors and showed that they generally perform better than spectral acceleration. Other researchers developed intensity indexes that consider spectral shape by means of the geometric mean of spectral acceleration at various periods, covering a wide spectral range (e.g., previous studies[20–23]). Marafi et al.[17] also proposed a new index that combines the spectral intensity, spectral shape and ground motion duration and demonstrated its efficiency in predicting the collapse of 30 MDOF structures.

In addition to spectral shape and strong motion duration, incremental velocity (IV)[24] has been recently identified by Dávalos and Miranda[25] as a parameter that influences the structural collapse. Sets of ground motions that need to be scaled by different factors to match a target spectral response at the fundamental period of selected SDOF and MDOF systems were assembled. The records were selected based on the approach proposed by Jayaram et al.[26] such that they also match a target conditional spectrum, in terms of their mean and variance. For all the examined structural models, the probability of collapse was shown to be larger when they were subjected to ground motions that required larger scale factors. It was also observed that these records were characterised by longer duration and larger IV accumulated in their 10 largest pulses, although their spectral shape did not differ from that of the rest of the accelerograms.

Although the effect of pulses on structural collapse capacity has been recognised, this has not been considered in studies dealing specifically with duration effects on collapse. Hence, there is a need to investigate the role of duration in structural collapse, with explicit consideration of the effect of pulses. In this study, the influence of duration on the collapse of ductile SDOF systems is quantified using two distinct approaches: (i) the method of spectrally equivalent records[12] and (ii) a novel procedure that ensures equivalence of ground motion records not only in terms of spectral shape but also in terms of IV. Based on the former method, a parametric assessment is performed, and design collapse capacity spectra are developed, with focus on the effects of duration in conjunction with other factors, including the period, negative postcapping stiffness, ductility capacity, strain hardening ratio and hysteretic behaviour. Beside spectral acceleration at the period of vibration, the influence of employing more advanced IMs that account for spectral shape, ground motion duration and acceleration pulses is examined in a comparative study. Finally, the proposed method is employed to reassess the role of duration in reducing the collapse capacity, using records that are equivalent both in terms of spectral shape and pulses.

2 | MODELLING PROCEDURES

2.1 | Structural represention

Since one of the main objectives of this study is to identify the key parameters influencing the collapse of ductile systems, a SDOF model with a trilinear backbone is employed to represent the lateral resisting system, which is adjusted according to the parameters considered. These parameters vary as indicated in Table 1 and include the period, the slope of the negative stiffness branch, the ductility and the strain hardening ratio. It should be noted that ductility herein refers to ductility capacity,[27] namely, the ratio of the displacement at which the negative stiffness branch begins to the yield displacement. Also, the strain hardening ratio refers to the stiffness of the intermediate branch of the system without gravity loading.

The SDOF system, which is illustrated in Figure 1 along with its moment-rotation curve, consists of a pinned rigid rod with a mass at its tip and a rotational spring and viscous damper at its base. The mass is tuned according to the period of the model, while Rayleigh damping $\xi = 5\%$ is assigned to the damper. A gravity load P is applied at the tip of the inverted pendulum, such that the desired level of P-Δ, as determined by the slope of the negative stiffness branch, is achieved. The postcapping stiffness of the system without gravity loads is set equal to $\alpha = 3\%$ of the initial elastic stiffness. Two types of hysteretic behaviour are examined; bilinear and pinching hysteresis without strength or stiffness degradation. The SDOF systems are modelled in OpenSees,[28] using the 'Steel01' and 'Pinching4' materials. The latter is

TABLE 1 Parameters defining the single-degree-of-freedom (SDOF) systems

Parameter	Values considered
Period, T (s)	0.2, 0.5, 0.7, 1.0, 2.0 and 3.0
Negative stiffness, θ-α	0.02, 0.04, 0.06, 0.10, 0.20 and 0.30
Ductility, μ_c	2.0, 4.0 and 6.0
Strain hardening ratio, α_h	0.00, 0.02, 0.05 and 0.10

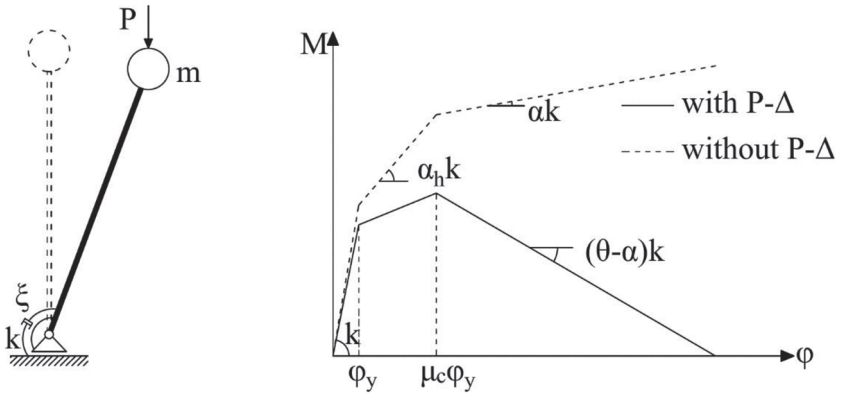

FIGURE 1 Single-degree-of-freedom (SDOF) system and backbone moment-rotation curves

defined based on energy damage and considering a moderate level of pinching (rDispP = rDispN = 0.1, fForceP = fForceN = 0.6, uForceP = uForceN = 0.0).

2.2 | Ground motion records

For the purpose of studying the ground motion duration effects, 101 pairs of short- and long-duration records with equivalent spectral response are assembled, according to the procedure outlined in Chandramohan et al.[12] Firstly, short and long records are selected from a wide database of past earthquakes. Events with 5–75% significant duration Ds_{5-75}[13] less than 25 s for both horizontal components of ground motion are considered as short, while the others are characterised as long. The records of the short set are subsequently scaled such that for each record of the long set, there is one scaled short record with equivalent 5% acceleration response spectrum. An upper limit of 5 is imposed on the required scale factor in order to avoid bias due to large scaling. Having eliminated any differences in spectral shape between pairs of short and long records, duration is assumed herein to be responsible for any differences in the response. However, this may not always hold true, as discussed in Section 7, where the influence of pulses is considered.

The geometric mean spectral response of the two sets is shown in Figure 2, while their distribution of duration is depicted in the form of histograms in Figure 3. It is noted that records with $Ds_{5-75} < 25$ s are included in the long-

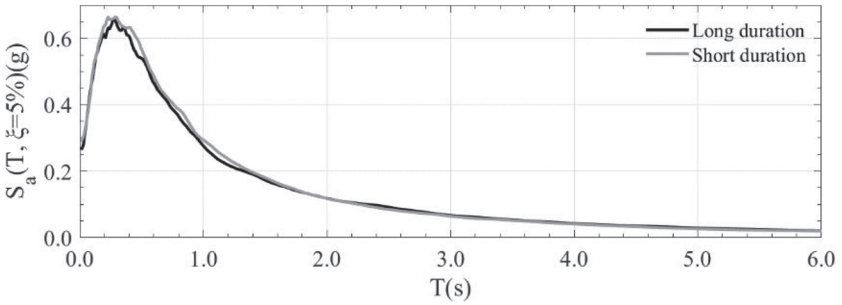

FIGURE 2 Geometric mean acceleration response spectra of long- and short-duration records

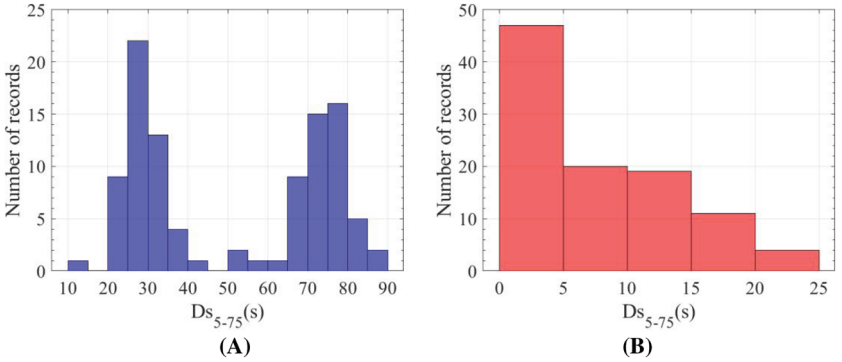

FIGURE 3 Distribution of 5–75% significant duration (Ds_{5-75}): A, long-duration set and B, short-duration set [Colour figure can be viewed at wileyonlinelibrary.com]

duration set, as they correspond to earthquakes for which the other horizontal component has a duration $Ds_{5-75} > 25$ s. Tables 2 and 3 show the events from which the short and long ground motion records are retrieved, respectively.

2.3 | Incremental dynamic analysis

Incremental dynamic analysis (IDA)[29] is employed for the collapse capacity assessment of the examined structural systems. Each record from the two sets is scaled to achieve increasing levels of intensity, as measured by means of the 5% spectral acceleration, up to collapse; at each of these levels, non-linear time history analysis is performed to determine the drift at the tip of the SDOF model. Through plotting the IM versus the engineering demand parameter (EDP), IDA curves are obtained. Flattening of the IDA curves or increase in drift above the maximum that the system can sustain are both considered to represent structural collapse. It is noted that the drift limit employed herein corresponds to the rotation for which the moment at the rotational spring of the SDOF is 0, based on its backbone curve. The spectral acceleration at the SDOF period $S_a(T)$ divided by the gravitational acceleration g and the base shear coefficient γ is employed as the IM, and the structural ductility μ is the EDP. The latter is defined as the ratio of the displacement at the tip of the SDOF system divided by its yield displacement and should not be confused with the ductility capacity μ_c, as defined in Section 2.1. The value of the IM at collapse, denoted as collapse capacity CC, is defined based on the spectral acceleration at the state of collapse $S_{ac}(T)$, as shown in Equation 1.[3] It is noteworthy that CC is equivalent to the collapse strength ratio R_c proposed by Miranda and Akkar.[2]

TABLE 2 Database of earthquakes for short-duration records

Earthquake	Number of records	Earthquake	Number of records
1999 Chi-chi, Taiwan	24	1981 Taiwan	3
1992 Cape Mendocino	1	2003 Big Bear City	1
1994 Northridge	8	1992 Erzican, Turkey	1
1986 Taiwan	1	2007 Chuetsu-oki	6
1999 Hector Mine	3	1984 Morgan Hill	2
2010 Darfield, New Zealand	3	1980 Irpinia, Italy	3
1989 Loma Prieta	2	2000 Yountville	1
1983 Coalinga	3	1997 Northwest China	1
2004 Niigata, Japan	2	2004 Parkfield	3
1983 Mammoth Lakes	1	1991 Sierra Madre	1
1979 Coyote Lake	2	1979 Imperial Valley	5
1987 Whittier Narrows	6	1995 Kobe, Japan	1
2008 Iwate	2	1992 Landers	4
1999 Kocaeli, Turkey	1	2010 El Mayor-Cucapah	2
2009 L'Aquila, Italy	1	1976 Friuli, Italy	1
1986 Chalfant Valley	2	1980 Livermore	1
1992 Cape Mendocino	1	2011 Christchurch	2

TABLE 3 Database of earthquakes for long-duration records

Earthquake	Number of records	Earthquake	Number of records
1985 Mexico City, Mexico	8	2010 El Mayor-Cucapah	6
1992 Landers	6	2010 Maule, Chile	16
1999 Kocaeli, Turkey	4	2011 Tohoku, Japan	49
2003 Hokkaido, Japan	12		

$$CC = \frac{S_{ac}(T)}{g\gamma} \tag{1}$$

Finally, the IDA curves of the long- and short-duration sets are extracted at their 50th, 16th and 84th fractiles, through finding the corresponding fractiles of drift at given levels of spectral acceleration. Accordingly, the 50%, 16% and 84% collapse capacities are obtained.

3 | PARAMETRIC ASSESSMENTS

A total of 864 SDOF systems subjected to 202 ground motion records were used in IDA in order to assess duration effects on collapse, in conjunction with other key parameters influencing ductile structures. The main results of the analyses are presented in the following, focusing primarily on the median IDA curves and the median collapse capacity, which are henceforth simply referred to as IDA curves and collapse capacity, respectively.

3.1 | IDA curves

The IDA curves under the short- and long-duration record sets for two of the examined SDOF models, namely, a bilinear and a pinching system with $T = 3.0$ s, θ-$\alpha = 0.06$, $\mu_c = 6.0$ and $\alpha_h = 0.05$, are shown in Figure 4A,B, respectively. After the end of the elastic stage, which is indicated by an intensity level of 1, the curves corresponding to short and long records start deviating from each other, ultimately reaching their capacities at different intensity levels. As expected, longer duration records lead to collapse under lower intensities compared with short ground motions. It is also observed that the duration-induced reduction of collapse capacity is relatively more pronounced in the case of bilinear compared with pinching hysteresis, which is discussed in detail in Section 4. Similar conclusions can be drawn for the other examined SDOF systems.

3.2 | Collapse capacity

This section focuses on the effect of the investigated structural parameters (period, slope of negative stiffness branch, ductility and strain hardening ratio) on collapse. Results are shown here only for bilinear systems for brevity, noting that pinching models are generally characterised by the same trends but higher collapse capacities.

Figure 5 illustrates the resulting collapse capacity under long and short ground motion records as a function of period and level of P-Δ for systems characterised by $\mu_c = 4.0$ and $\alpha_h = 0.02$. It is noticeable that the first-mode period plays a major role, provided that second-order effects are kept at low levels, in which case more than three times higher collapse capacity is obtained as the period increases from 0.2 to 3.0 s. On the other hand, the capacity becomes practically insensitive to the SDOF period for systems with relatively high levels of P-Δ (θ-$\alpha = 0.2$ and θ-$\alpha = 0.3$). This can be explained by the fact that once such systems enter the postcapping range, they collapse almost immediately, with a collapse capacity close to unity irrespective of other parameters (including ground motion duration). With respect to the

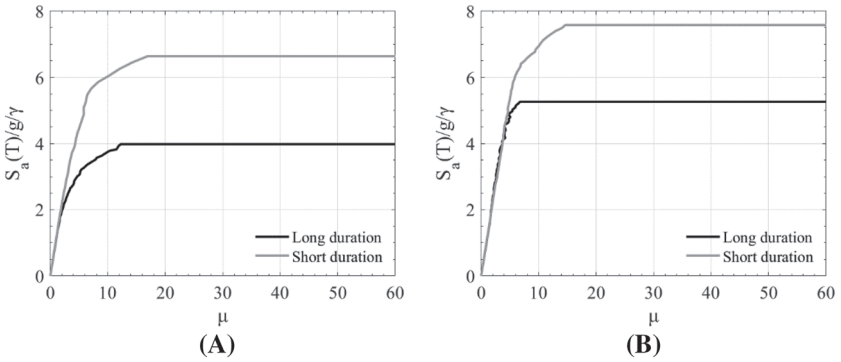

FIGURE 4 Incremental dynamic analysis (IDA) curves under short- and long-duration records for a system with $T = 3.0$ s, θ-$\alpha = 0.06$, $\mu_c = 6.0$, $\alpha_h = 0.05$ and A, bilinear hysteresis and B, pinching hysteresis

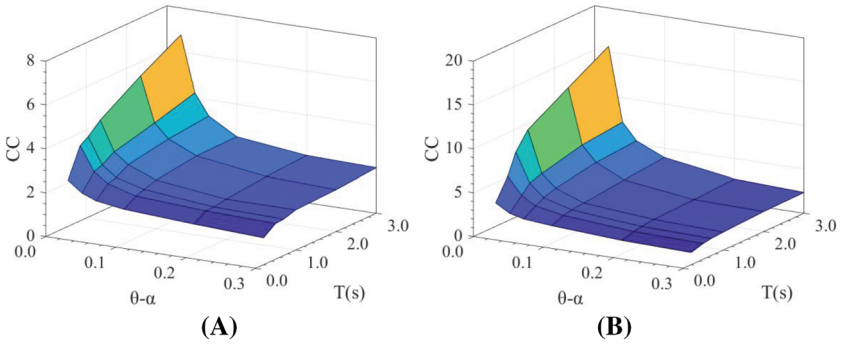

FIGURE 5 Effect of period and level of *P*-Δ on the collapse capacity for systems with $\mu_c = 4.0$, $\alpha_h = 0.02$ and bilinear hysteresis, subjected to A, long-duration records and B, short-duration records [Colour figure can be viewed at wileyonlinelibrary.com]

influence of *P*-Δ, the collapse intensity tends to decrease rapidly as the level of *P*-Δ increases, reaching a minimum at θ-$\alpha = 0.2$, from which level onwards it remains almost unchanged. It is noted, however, that the effect of *P*-Δ attenuates with decreasing levels of period. In other words, the response of rigid structures is not affected by other parameters, similarly to what was observed for systems affected by high levels of *P*-Δ. These conclusions regarding the detrimental role of the stiffness of the backbone decreasing branch and the beneficial effect of period have been well documented in the literature.[2,3,5,15]

Turning to the effect of ductility and strain hardening ratio on collapse, Figure 6 depicts the variation of collapse capacity as a function of these two factors for SDOFs with $T = 0.5$ s and θ-$\alpha = 0.02$ subjected to long- and short-duration earthquake records. Strain hardening ratio is shown to be beneficial to the system's capacity, with its effect being more pronounced at high levels of ductility. Regarding the role of ductility, it can be either favourable or detrimental, depending on the value of strain hardening ratio compared with the rotation of the force-deformation curve due to *P*-Δ effects. In cases that the former is higher or equal to the latter (i.e., $\alpha_h \geq \theta$), the stiffness of the intermediate branch of the static pushover curve after the application of gravity loads remains positive or equal to zero, which implies that this branch contributes to collapse resistance. Therefore, higher ductility results in longer intermediate branch and hence higher collapse capacity. On the contrary, the opposite holds true if the rotation caused by *P*-Δ is large enough to cause a negative slope of the intermediate branch (i.e. $\alpha_h < \theta$), thus turning its influence to be adverse, where a decreasing trend of collapse capacity with ductility is noticed. These observations are consistent with those made by Vamvatsikos et al.[5] who considered SDOFs with positive stiffness of the intermediate branch and reported a positive influence of ductility irrespective of strain hardening.

3.3 | Dispersion of results

The median collapse capacity, which was examined in Section 3.2, does not offer any information on the variability in collapse capacity due to individual record characteristics. This additional information can be obtained by a measure of dispersion, which is of great importance within the context of probabilistic performance-based design. If the common assumption that collapse capacities follow a lognormal distribution is adopted (e.g., Ibarra and Krawinkler[27]), then the geometric standard deviation, $\sigma_{g\ CC}$, is a suitable measure of the variability. The latter is indeed independent of the mean of the distribution, thus allowing efficient comparison of dispersion of the SDOF systems considered in this study. As the lognormal distribution is only an approximation, computation of the geometric standard deviation as the ratio of

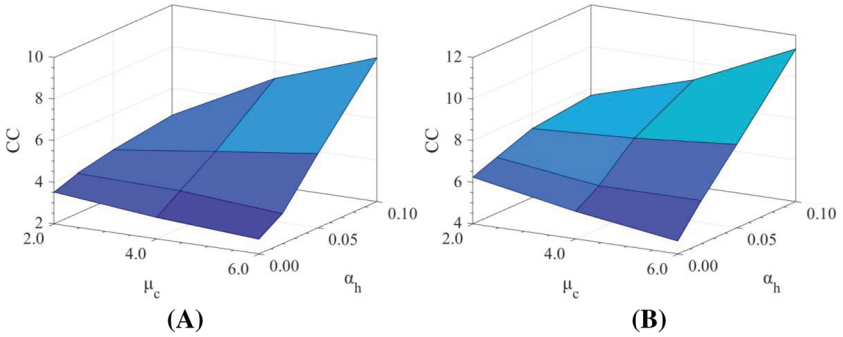

FIGURE 6 Effect of ductility and strain hardening ratio on the collapse capacity for systems with $T = 0.5$ s, θ-$\alpha = 0.02$ and bilinear hysteresis, subjected to A, long-duration records and B, short-duration records [Colour figure can be viewed at wileyonlinelibrary.com]

the 16th to 50th capacity fractiles results in slightly different estimations than if the 50th and 84th fractiles are used. The results presented herein are based on the former definition.

Firstly, the effect of the system parameters is examined focusing on bilinear hysteresis. Collapse capacity dispersion is plotted in Figure 7A against P-Δ for each level of period and fixed ductility and strain hardening ratio ($\mu_c = 2.0$ and $\alpha_h = 0.00$). A reduction in collapse variability is observed with a decrease of period or increase of P-Δ, both of which result in reduction of collapse capacity and, hence, trimming of the spread around the median. This holds true for both long and short records, except that in the former case, the level of P-Δ does not seem to have a notable effect. Figure 7B shows the role of hardening and ductility for systems with $T = 3.0$ s and θ-$\alpha = 0.06$, based on which it can be argued that collapse capacity dispersion depends only to a limited extent on these two factors.

From Figure 7, it becomes clear that collapse capacity dispersion reduces with increasing ground motion duration. In order to investigate the influence of duration in more detail and illustrate the differences between the two types of hysteresis, histograms of the dispersion are plotted in Figure 8 for each duration group and hysteretic behaviour.

It can be noticed that long-duration earthquakes are associated, on average, with lower collapse capacity dispersion compared with shorter seismic events. In addition, the distribution of dispersion under short records is more uniform, covering a wider range of values. The reason for this difference is that long records result in lower collapse capacities and, hence, the variation due to record-to-record variability is expected to be lower. On the other hand, large collapse capacities occur under short ground motions, in which case the ratio of 16th to 50th fractiles of collapse capacity can be as high as about 2.80. Comparison of Figure 8A,B reveals that the collapse capacity dispersion of pinching systems tends to be concentrated at a narrower range than in the case of bilinear systems. It is also worth noting that the lowest levels of dispersion are obtained for bilinear systems subjected to long records.

3.4 | Collapse fragility curves

In order to verify the validity of the assumed lognormal distribution of collapse capacity, collapse fragility curves, as obtained by the statistical population of collapse capacities due to each record, are compared with fitted lognormal cumulative distribution functions. Figure 9 plots both types of fragility curves for two of the examined SDOFs (bilinear and pinching system with $T = 3.0$ s, θ-$\alpha = 0.06$, $\mu_c = 6.0$ and $\alpha_h = 0.05$) subjected to the long- and short-duration sets. The counted and fitted curves match closely in all cases, which implies that the assumption of lognormal distribution is reasonable. The larger vulnerability to collapse under longer earthquakes is also readily confirmed.

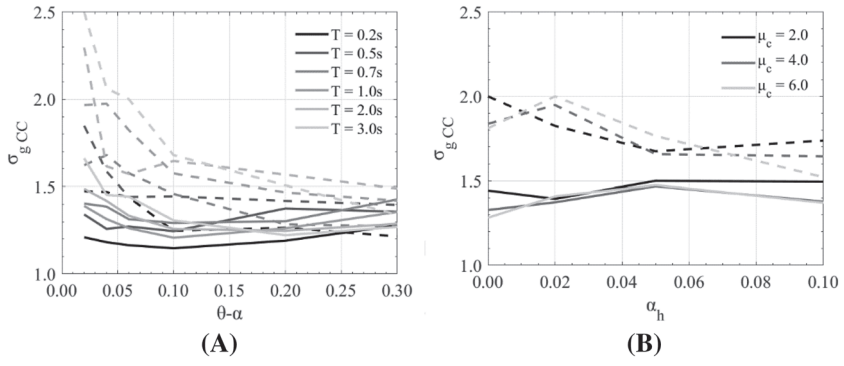

FIGURE 7 Collapse capacity dispersion as a function of A, level of P-Δ for systems with variable T, $\mu_c = 2.0$ and $\alpha_h = 0.00$ and B, strain hardening ratio for systems with variable μ_c, $T = 3.0$ s and θ-$\alpha = 0.06$. Both subfigures refer to bilinear hysteresis and long (solid lines) and short (dashed lines) ground motion sets

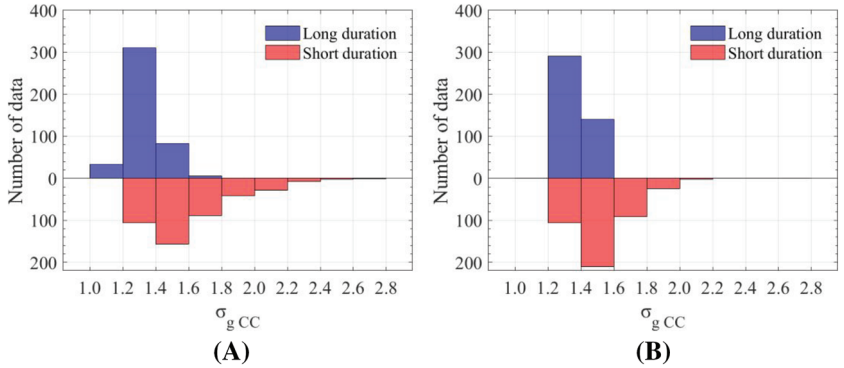

FIGURE 8 Histograms of collapse capacity dispersion of systems with A, bilinear hysteresis and B, pinching hysteresis, subjected to long- and short-duration records [Colour figure can be viewed at wileyonlinelibrary.com]

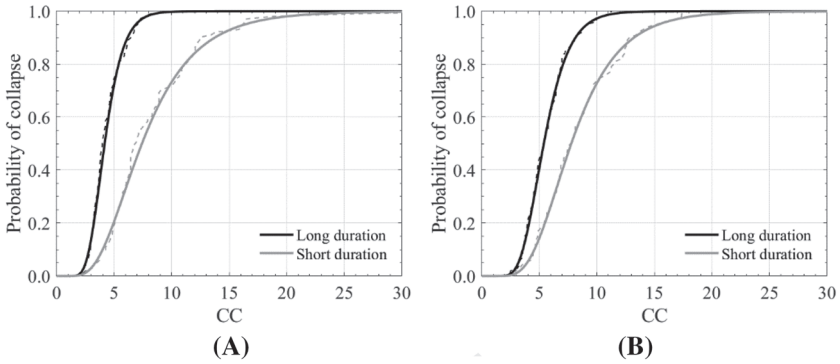

FIGURE 9 Counted (dashed lines) and fitted lognormal (solid lines) collapse fragilities under short- and long-duration records for a system with $T = 3.0$ s, θ-$\alpha = 0.06$, $\mu_c = 6.0$, $\alpha_h = 0.05$ and A, bilinear hysteresis and B, pinching hysteresis

4 | DURATION EFFETCS

Based on the results from the previous section, the percentage reduction in collapse capacity due to duration is computed herein, in order to provide a direct comparison of the response under short and long records. The collapse capacity reduction is plotted in Figures 10 and 11 against the main parameters examined. More specifically, Figure 10A,B shows the influence of period and P-Δ for bilinear systems with fixed ductility $\mu_c = 4.0$ and strain hardening ratio $\alpha_h = 0.00$ and pinching systems with $\mu_c = 6.0$ and $\alpha_h = 0.10$, respectively. It is noted that these values of ductility and strain hardening are selected such that the collapse capacity reduction is maximised for each hysteretic model considered. The effect of these two parameters on the duration-induced capacity reduction is shown in Figure 11A,B for bilinear and pinching systems, respectively, with $T = 3.0$ s and θ-$\alpha = 0.02$.

From Figures 10 and 11, it can be concluded that the effect of duration on collapse mainly depends on the period, the level of P-Δ and the hysteretic behaviour, while ductility and strain hardening seem to be of minor importance. Duration effects become increasingly significant as the period increases or the level of P-Δ reduces. This can be attributed to the increase in collapse resistance for systems with high levels of period or low levels of P-Δ, which can endure many inelastic cycles before their capacity is exhausted, thus resulting in different response due to strong motion duration. Therefore, noticeable reductions in collapse capacity are obtained under long records compared with short cases. In contrast, extremely rigid structures or those vulnerable to second-order effects tend to collapse almost immediately once they enter the inelastic range without being exposed to many inelastic cycles. Accordingly, their collapse capacity is close to unity irrespective of ground motion duration. With respect to the influence of hysteresis, duration appears to

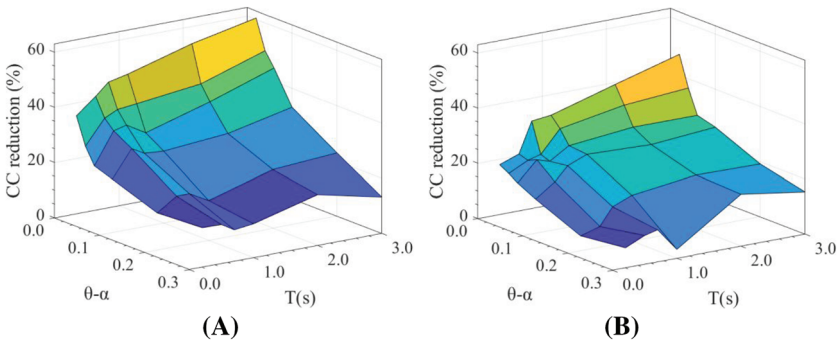

FIGURE 10 Effect of period and level of P-Δ on collapse capacity reduction due to duration for systems with A, $\mu_c = 4.0$, $\alpha_h = 0.00$ and bilinear hysteresis and B, $\mu_c = 6.0$, $\alpha_h = 0.10$ and pinching hysteresis [Colour figure can be viewed at wileyonlinelibrary.com]

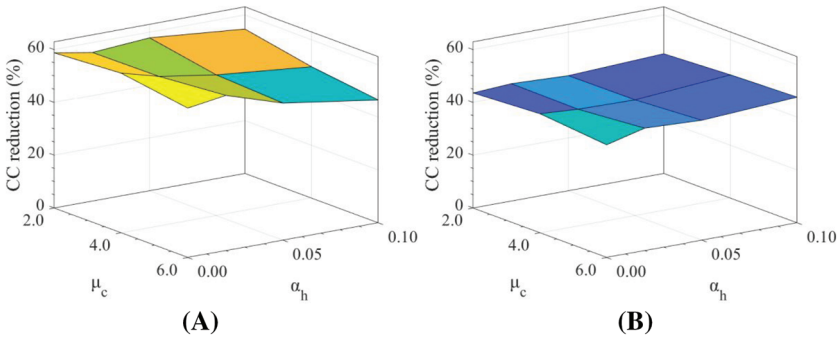

FIGURE 11 Effect of ductility and strain hardening ratio on collapse capacity reduction due to duration for systems with A, $T = 3.0$ s, θ-$\alpha = 0.02$ and bilinear hysteresis and B, $T = 3.0$ s, θ-$\alpha = 0.02$ and pinching hysteresis [Colour figure can be viewed at wileyonlinelibrary.com]

be more important for bilinear systems, being responsible for a reduction of up to 61% in collapse capacity, compared with a maximum of 48% in the case of pinching models. Considering that the main difference between the two hysteresis models is the longer length of the 'inner loops' in the case of pinching hysteresis,[30] it explains why the latter are less prone to duration. The longer the 'inner loops' are, the more the transition to the outer part of the curve, where the stiffness is negative, is delayed, and, hence, the less vulnerable the system is expected to be to longer duration earthquakes. It should also be noted that the distinct hysteretic energy dissipated in the two models cannot explain the larger effect of duration in bilinear systems, based on preliminary analyses that have been performed.

5 | COLLAPSE CAPACITY SPECTRA

The IDA results are processed in this section in order to develop appropriate formulae that can reproduce the collapse capacities for each type of ground motion duration based on key properties of the SDOF systems. To this end, nonlinear regression analyses are carried out for each duration set and hysteresis model. Except for the quality of curve fitting, simplicity is also an important criterion in choosing the best functional form. In addition, care is taken to satisfy the constraint that the collapse capacity of rigid systems should be unity, that is, $CC(T = 0\text{ s}) = 1.0$.[4] The developed formulae also incorporate the expressions for collapse capacity spectra of nonductile systems presented in Bravo-Haro et al.[15] so that collapse capacities are accurately recovered for $\mu_c = 1.0$. These expressions are modified as shown in Equation 2, in order to reduce the complexity of the final formulae, but without significant loss of accuracy.

$$CC_{\mu_c=1} = 1 + m_1\left(m_2 + e^{m_3 T}\right) T^{m_4} (\theta - \alpha)^{m_5 + m_6 \ln(T)} \tag{2}$$

After testing different functional forms, Equation 3 is derived, which gives the collapse capacity CC of a system with period T, level of P-Δ, θ-α, ductility μ_c and strain hardening ratio α_h as a function of the collapse capacity of the corresponding nonductile system $CC_{\mu_c=1}$.

$$\frac{CC}{CC_{\mu_c=1}} = 1 + T^{k_1}\left({\mu_c}^{k_2} - 1\right)(\alpha_h + k_3)\left[k_4(\theta - \alpha) + e^{k_5 T}\right] \tag{3}$$

The coefficients m_1–m_6 and k_1–k_5 are given in Table 4 for the 16%, 50% and 84% collapse capacity spectra of bilinear and pinching systems.

TABLE 4 Regression coefficients for 16%, 50% and 84% collapse capacity spectra for bilinear and pinching systems under long- and short-duration records

	Bilinear						**Pinching**					
	Long			**Short**			**Long**			**Short**		
	16%	**50%**	**84%**	**16%**	**50%**	**84%**	**16%**	**50%**	**84%**	**16%**	**50%**	**84%**
m_1	1.099	0.571	0.141	1.272	0.548	0.404	1.099	0.571	0.141	1.272	0.548	0.404
m_2	0.219	0.239	0.554	0.130	0.211	0.275	0.219	0.239	0.554	0.130	0.211	0.275
m_3	−1.620	−1.364	−0.763	−1.767	−1.458	−1.751	−1.620	−1.364	−0.763	−1.767	−1.458	−1.751
m_4	0.486	0.678	0.599	0.590	0.617	0.618	0.486	0.678	0.599	0.590	0.617	0.618
m_5	−0.623	−0.663	−0.761	−0.940	−0.890	−0.809	−0.623	−0.663	−0.761	−0.940	−0.890	−0.809
m_6	−0.142	−0.078	−0.046	−0.202	−0.136	−0.102	−0.142	−0.078	−0.046	−0.202	−0.136	−0.102
k_1	0.071	0.079	0.032	0.233	0.131	0.260	0.071	0.079	0.032	0.233	0.131	0.260
k_2	1.792	1.676	1.522	1.451	1.409	1.486	1.792	1.676	1.522	1.451	1.409	1.486
k_3	−0.021	−0.024	−0.028	−0.012	−0.021	−0.029	−0.021	−0.024	−0.028	−0.012	−0.021	−0.029
k_4	−3.107	−3.463	−3.760	−1.643	−1.902	−2.098	−3.107	−3.463	−3.760	−1.643	−1.902	−2.098
k_5	−0.053	0.008	0.065	−0.101	0.024	−0.115	−0.053	0.008	0.065	−0.101	0.024	−0.115

Design collapse capacities, as predicted by Equation 3, are plotted in Figures 12 and 13 for bilinear and pinching systems, considering both long and short ground motion duration. Figure 12 shows collapse capacity spectra for various levels of P-Δ and fixed ductility and strain hardening ($\mu_c = 4.0$ and $\alpha_h = 0.02$). Typical trends described in Section 3.2, such as the increase of collapse capacity with decreasing P-Δ effects and increasing period, are accurately represented by the proposed expressions, while collapse capacities for long-duration records are below those correspoding to short ground motions, as expected. In Figure 13, design collapse capacities are plotted against ductility for various levels of strain hardening ratio, while the period of vibration and the P-Δ effect are kept constant ($T = 0.5$ s and θ-$\alpha = 0.04$). Again, the increasing trend of collapse capacity with strain hardening and the effect of ductility, which depends on the strain hardening ratio, are accurately captured by the suggested formulae.

The accuracy of the developed design spectra can be verified by means of statistical indices, such as the mean-square error (MSE), which is kept at relatively low levels for all examined hysteresis and duration groups, as shown in Table 5. The MSE is higher for the 16% design spectra, followed by the median and the 84% spectra, which reflects the ranking of 16%, 50% and 84% collapse capacities. Similarly, short ground motions are related to greater values of MSE, as the collapse capacity data in the short-duration set are higher than those corresponding to long duration.

The predicted collapse capacities according to Equation 3 are plotted against the observed values from the analyses for pinching models in Figure 14, in order to visualise the data and ensure the accuracy of the models. As shown in the figure, there is a good agreement between the predictions and the observations, since the data points are closely correlated. In addition, the variance of the data (i.e., their scatter around the diagonal) does not change significantly with the predicted collapse capacity, which indicates that the residuals are homoscedastic. It is noted that similar results can be obtained for bilinear systems. As further verification of the suitability of the proposed expressions, design collapse capacity spectra are plotted along with the values of collapse capacity obtained from the analyses in Figure 15, which refers to bilinear systems with fixed levels of ductility and strain hardening ($\mu_c = 4.0$ and $\alpha_h = 0.05$).

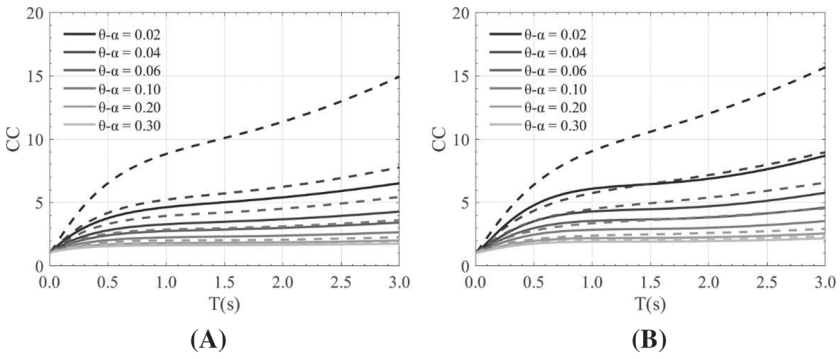

FIGURE 12 Design collapse capacity spectra for long (solid lines) and short (dashed lines) ground motion duration for systems with variable θ-α, $\mu_c = 4.0$, $\alpha_h = 0.02$ and A, bilinear hysteresis and B, pinching hysteresis

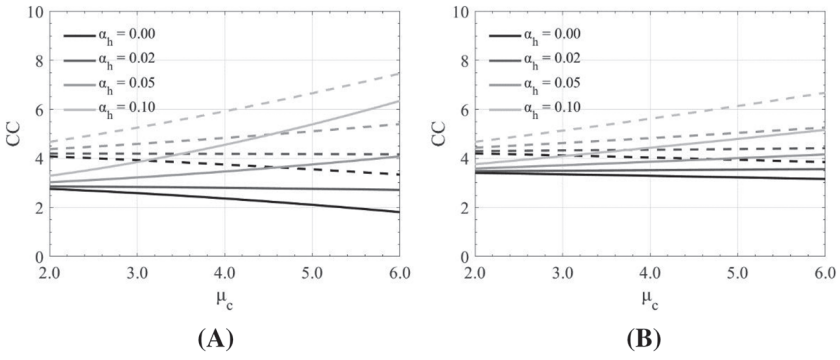

FIGURE 13 Design collapse capacity spectra for long (solid lines) and short (dashed lines) ground motion duration for systems with variable α_h, $T = 0.5$ s, θ-$\alpha = 0.04$ and A, bilinear hysteresis and B, pinching hysteresis

TABLE 5 Mean-square error of 16%, 50% and 84% design collapse capacity spectra for bilinear and pinching systems subjected to long- and short-duration records

	Long			Short		
	16%	50%	84%	16%	50%	84%
Bilinear	0.345	0.105	0.041	1.139	0.147	0.037
Pinching	0.096	0.041	0.020	0.261	0.098	0.036

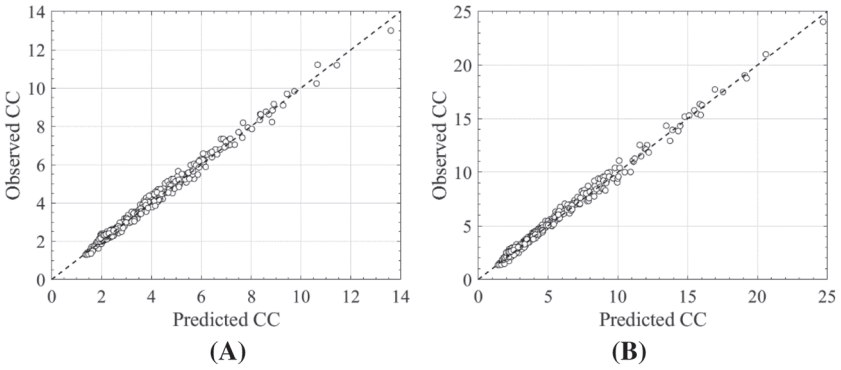

FIGURE 14 Observed versus predicted values of collapse capacity for pinching systems subjected to A, long-duration records and B, short-duration records

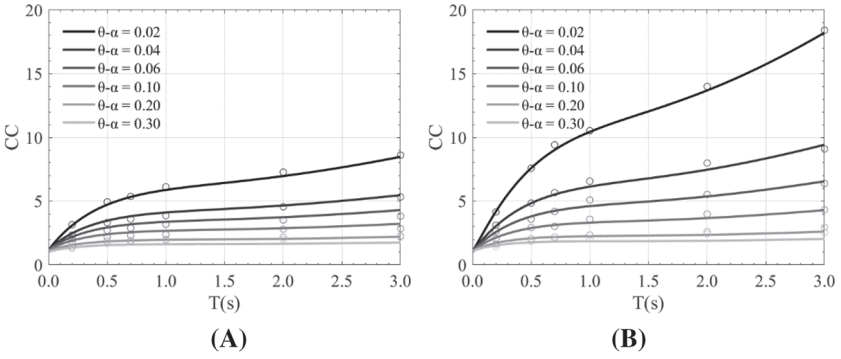

FIGURE 15 Design collapse capacity spectra and collapse capacities obtained from incremental dynamic analysis (IDA) for bilinear systems with variable θ-α, $\mu_c = 4.0$, $\alpha_h = 0.05$ subjected to A, long-duration records and B, short-duration records

Finally, the collapse capacity spectra derived herein are compared with analogous expressions presented by Han et al.[6] who investigated the seismic collapse of a series of bilinear SDOF systems with varying period, damping ratio, hardening stiffness, negative slope stiffness and ductility. With respect to the SDOF models employed, a trilinear backbone curve with negative stiffness in the third branch was considered, without applying any gravity loads. This is in contrast to the present study, where the P-Δ effect is explicitly accounted for by means of gravity loading at the tip of the SDOF, which causes a rotation of the backbone. In the following comparisons, the negative stiffness slope employed by Han et al.[6] is considered equal to the value of θ-α used in this study.

The median collapse capacities based on Equation 3 for both types of hysteresis and ground motion duration, as well as those computed according to Han et al.[6] are plotted against the structural period in Figure 16 for low (θ-$\alpha = 0.04$) and high (θ-$\alpha = 0.30$) level of P-Δ. It is noted, however, that only the spectra for bilinear hysteresis are comparable with those derived by Han et al.[6] which also refer to bilinear, ductile systems.

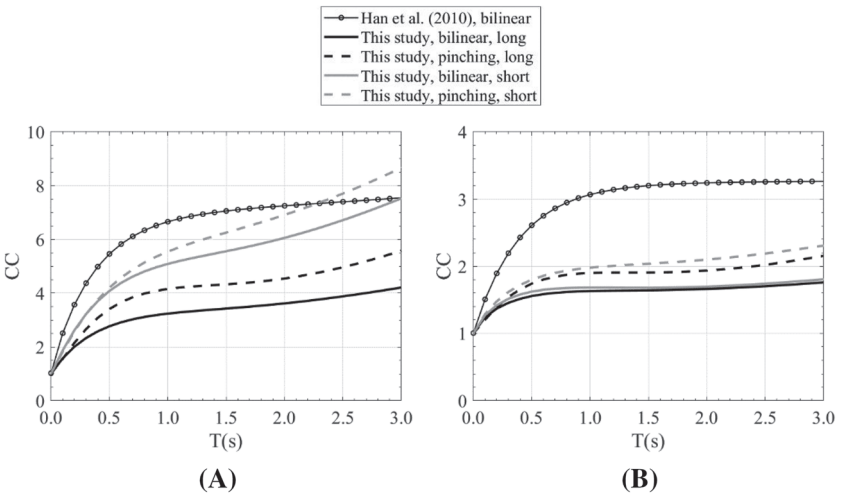

FIGURE 16 Comparison of collapse capacity spectra from this study with the expressions derived by Han et al.[6] for systems with $\mu_c = 2.0$, $\alpha_h = 0.00$ and A, θ-$\alpha = 0.04$ and B, θ-$\alpha = 0.30$

According to Figure 16A, the predicted values of collapse capacity based on Han et al.[6] are in relatively good agreement with those obtained from this study for bilinear systems under short-duration records. However, the capacity is significantly reduced for long ground motion duration, resulting in nonnegligible differences between the two studies in the case of longer earthquakes. This indicates the necessity of accounting for duration effects in the assessment of collapse resistance. Figure 16B, on the other hand, shows that the agreement between the present work and Han et al.[6] deteriorates for higher levels of θ-α. This can be explained considering that the two studies are not directly comparable due to the different approach in accounting for the P-Δ effect and defining the backbone curve (through application of gravity loading or not). It is also noted that that this difference is more important for high levels of P-Δ. In addition, the spectra under short and long records almost coincide, since ground motion duration is not important for high levels of P-Δ, as discussed in Section 4.

6 | ALTERNATIVE IMS

In the previous sections, the collapse capacity CC,[3] which is proportional to spectral acceleration at the period of vibration as described in Equation 1, was employed to quantify the ground motion intensity that causes structural collapse. Evidently, this IM contains information on the amplitude at one specific period but provides no insight into other characteristics, such as spectral shape or duration. The influence of the former has been examined in previous studies (e.g., Eads et al.[22]), while this study, along with past research (e.g., Chandramohan et al.[12]), proves the importance of the latter. Due to its disregard of other significant features of the ground motion, spectral acceleration can lead to relatively high levels of dispersion at collapse, as shown in Section 3.3, thus making it necessary to run analyses for a large number of records in order to obtain stable estimates of structural response. As a result, more advanced IMs have been proposed in the literature, which aim at minimising this deficiency.

Among the available IMs, S^*,[18] Sa_{avg}[22] and IM_{comb}[17] are investigated herein, focusing on their efficiency, that is, their ability to reduce dispersion at collapse. The first two account for the influence of spectral shape, while the third considers in addition the strong motion duration, as can be observed by their definitions given in Equations 4–6 as follows:

$$S^* = S_a(T)\sqrt{\frac{S_a(2T)}{S_a(T)}}, \tag{4}$$

$$Sa_{avg} = \left(\prod_{i=1}^{N} S_a(T_i)\right)^{1/N}, \; T_{i=1} = 0.3T, \; T_{i=N} = 2T, \tag{5}$$

$$IM_{\text{comb}} = S_a(T) Ds_{5-95}{}^{C_{\text{dur}}} SS_{\text{a}}(T,a)^{C_{\text{shape}}}, \quad a = C_a\sqrt{\mu} = 1.3\sqrt{\mu}, \tag{6}$$

where S_a is the spectral acceleration, T is the SDOF period, Ds_{5-95} is the 5–95% significant duration, SS_a is a measure of spectral shape,[17] μ is the structural ductility and C_{dur} and C_{shape} are empirical exponents that are optimised to give the lowest possible dispersion for IM_{comb} at collapse.[17] It should be noted that Sa_{avg} is computed herein using 100 values of spectral acceleration at uniformly spaced periods from 0.2 T to 3.0 T, as recommended by Eads et al.[22] who found that this period range resulted in relatively low dispersion at collapse, based on analysis results of almost 700 MDOFs. Optimisation of the period range for each SDOF system is out of the scope of this study and is not expected to lead to significant improvement in terms of efficiency.

Beside spectral shape and duration, a recent study by Dávalos and Miranda[25] has shown that acceleration pulses of ground motion could also influence the collapse potential. Based on this observation, four variations of IM_{comb} are investigated herein, in order to assess whether their inclusion could improve the IM's efficiency. More specifically, IM_1 accounts for the effect of pulses, ignoring duration, while IM_2 considers both these ground motion characteristics. IM_3 and IM_4 employ Sa_{avg} instead of SS_a as a measure of spectral shape and include acceleration pulses and duration, respectively. The effect of pulses is quantified by means of the maximum incremental velocity,[24] IV_{max}, which is defined as the increment of velocity corresponding to the pulse with the largest area. These four IMs are defined by Equations 7–10 as follows:

$$IM_1 = S_a(T) IV_{\max}{}^{C_{\text{pulses}}} SS_a(T,a)^{C_{\text{shape}}}, \tag{7}$$

$$IM_2 = S_a(T) Ds_{5-95}{}^{C_{\text{dur}}} SS_a(T,a)^{C_{\text{shape}}} IV_{\max}{}^{C_{\text{pulses}}}, \tag{8}$$

$$IM_3 = Sa_{\text{avg}} S_a(T)^{C_{Sa}} IV_{\max}{}^{C_{\text{pulses}}}, \tag{9}$$

$$IM_4 = Sa_{\text{avg}} S_a(T)^{C_{Sa}} Ds_{5-95}{}^{C_{\text{dur}}}, \tag{10}$$

where $IV_{\max}$ is the maximum incremental velocity and C_{pulses} and C_{Sa} are empirical exponents that are optimised to give the lowest possible dispersion, similarly to C_{dur} and C_{shape}.

The dispersion of collapse estimates obtained using the above-mentioned IMs is quantified based on the assumption of lognormal distribution by means of geometric standard deviation, $\sigma_{\text{g IM}}$, as discussed before in Section 3.3. The resulting levels of dispersion for each combination of hysteresis model and strong motion duration are presented in Figures 17 and 18, in the form of box plots.

Based on Figures 17 and 18, it is evident that CC is the least efficient IM, since it exhibits higher dispersion than the other IMs, in terms of median, minimum and maximum values, except for bilinear systems under long-duration records, in which case its performance is comparable with that of Sa_{avg} and S^*. Among the first four IMs, IM_{comb} appears to be superior, providing the lowest deviation of collapse estimates. These observations are in close agreement with those of other researchers, such as Marafi et al.[17] and Eads et al.[22] Nevertheless, since a relatively large number of records was used, the choice of CC as the IM is deemed to lead to stable collapse estimates, while it is also a simple and commonly employed intensity index.

Comparison of IM_{comb}, IM_1, and IM_2 reveals that inclusion of IV does not lead to improvement of efficiency compared with the case of considering only duration and spectral shape. If, however, spectral shape is considered by means of Sa_{avg} and IV is also taken into account, then some enhancement of performance is noticed in the case of short-duration records. Indeed, IM_3 offers the lowest median dispersion and limits the range of variation of dispersion at collapse compared with other IMs for bilinear and pinching systems subjected to short records. Replacement of IV with significant duration yields slightly higher dispersions, as shown by IM_4. Nevertheless, the differences among the IMs that account either for duration or IV are relatively small and neither of these two parameters can be argued to outperform the other.

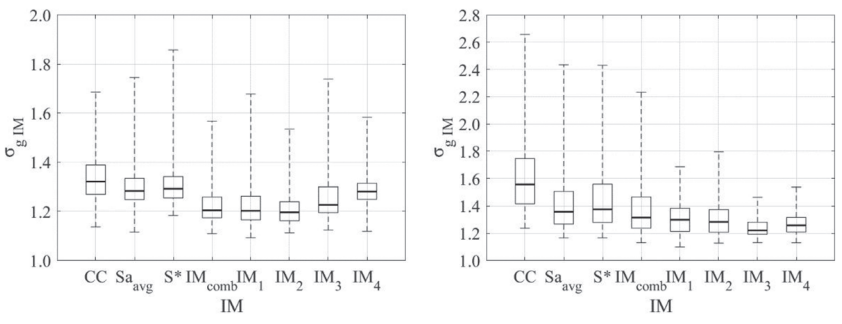

FIGURE 17 Box plots of dispersion of intensity measures (IMs) at collapse for bilinear systems subjected to A, long-duration records and B, short-duration records. Bold lines show medians; bottom and top edges of boxes correspond to first and third quartile, respectively; lines at ends of whiskers refer to minimum and maximum dispersions

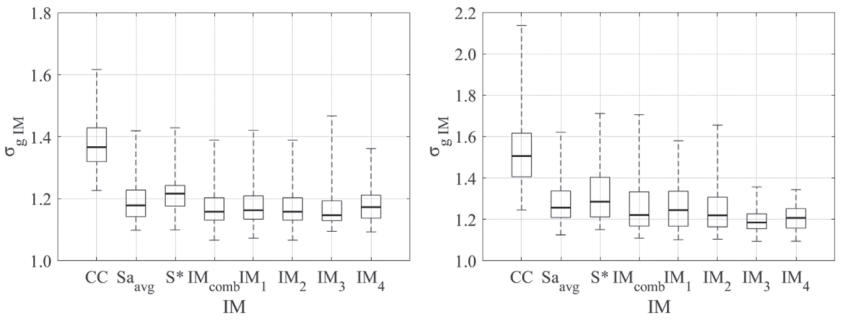

FIGURE 18 Box plots of dispersion of intensity measures (IMs) at collapse for pinching systems subjected to A, long-duration records and B, short-duration records. Bold lines show medians; bottom and top edges of boxes correspond to first and third quartile, respectively; lines at ends of whiskers refer to minimum and maximum dispersions

7 | INFLUENCE OF PULSES

As mentioned previously, acceleration pulses of ground motion have been recently identified as a potentially significant factor influencing the collapse capacity of structures.[25] Hence, a complete investigation of duration effects on seismic collapse is only possible if all other characteristics of the strong motion records are kept constant, including acceleration pulses. The method of spectrally equivalent records[12] followed in this paper accounts for amplitude and spectral shape and assumes that if these parameters are fixed then any observed differences in response between the sets of long and short records can be attributed to duration, thus ignoring the role of pulses. However, if the differences in terms of pulses between the two sets are important, then some bias in the recorded duration effects might be expected. This section therefore focuses on this issue and examines whether it is crucial in determining the influence of strong motion duration on collapse.

7.1 | IV characteristics

The effect of pulses is quantified herein by means of the IV, which is defined as the difference of peak velocities of two consecutive velocity pulses or, in an equivalent manner, the area under the corresponding acceleration pulse.[24] Mean IVs of the two sets of records, sorted in decreasing order, are plotted in Figure 19A, while Figure 19B isolates the first 10 pulses, which are expected to influence mostly the response.[25] Evidently, IV attenuates more rapidly in the case of short rather than long-duration records, as a result of the fewer pulses of short earthquakes. Focusing on the first 10 pulses (Figure 19B), it can be argued that, on average, short records tend to have higher IV for the first two pulses, but this is reversed after the third pulse, with long records exhibiting higher levels of IV, which is more slowly decaying compared with their short counterparts. Although it may be surprising that the mean maximum IV of the short and long sets do not differ significantly, it should be noted that these are mean values and greater differences may arise if individual short records are set in contrast to their long, spectrally equivalent, counterparts. In addition, relatively small differences between the maximum IV of short and long records have also been reported in previous studies (e.g., Kohrangi et al.[31]).

Figure 20A depicts the cumulative sum of IVs, ΣIV, of long and short earthquakes, with the first 10 pulses shown separately in Figure 20B. As expected, the curve that corresponds to short earthquakes, saturates at around the 200th pulse, from which point onwards there are, on average, almost no more pulses with considerable IV embedded in short

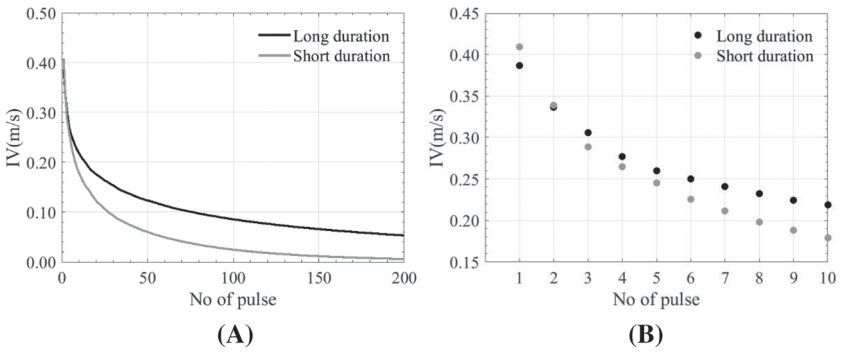

FIGURE 19 Mean incremental velocity (IV) in long and short-duration records versus pulse number for A, first 200 pulses and B, first 10 pulses

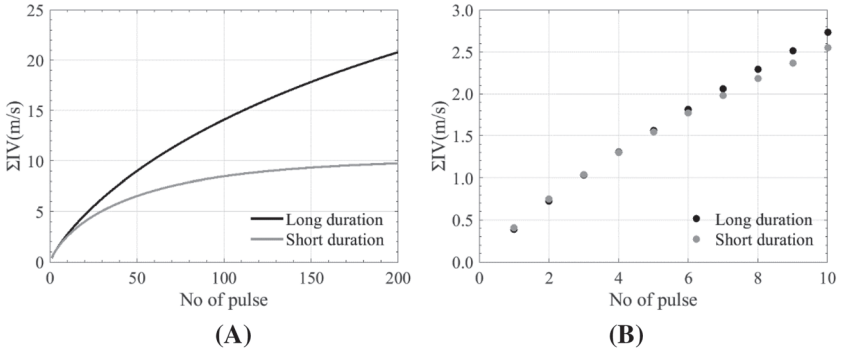

FIGURE 20 Mean cumulative incremental velocity (ΣIV) in long- and short-duration records versus pulse number for A, first 200 pulses and B, first 10 pulses

records. After the first couple of pulses, the two curves corresponding to long and short ground motions deviate from each other, with their differences becoming increasingly important as short-duration records exhibit a milder rate of increase of ΣIV. From Figure 20B, it is observed that short records tend to be more significant than their long counterparts for the first few pulses, but the latter then dominate after the fifth pulse.

Based on Figures 19 and 20, it can be concluded that the acceleration pulses of the 101 long- and 101 short-duration records employed herein are not characterised by the same average trends. In fact, even higher differences in terms of IV between the individual pairs of spectrally equivalent records may be observed. Accordingly, these sets of records are not equivalent in terms of pulses, which warrants further investigation.

7.2 | Equivalence procedures

In order to isolate duration effects, two sets of long and short records that are equivalent in terms of amplitude, spectral shape and IV need to be assembled. Since the records used herein are characterised by different IVs, each long record is modified such that the IVs of the first 10 pulses are matched to those of its spectrally equivalent short counterpart. This is achieved through an iterative process, as depicted in Figure 21.

After determining the 10 greatest pulses of each long record and those of the corresponding response spectrally equivalent short event, the acceleration data of each pulse of the long-duration records are adjusted such that the area under the pulse corresponds to the target IV. If, however, this adjustment results in a change of sign of the acceleration, then a small value of acceleration with the same sign is considered instead, in order to avoid the emergence of new pulses. It is noted that the term 'pulse' refers to part of the accelerogram between two consecutive zero-crossings. The adjustment procedure terminates when a predefined level of tolerance is reached. In case that another pulse becomes critical (i.e., its IV exceeds the IV of the adjusted pulse), the procedure is repeated for the new critical pulse. At the end of this modification, the 10 greatest pulses of the long-duration records are matched to those of their response spectrally equivalent short counterparts.

Because this algorithm can cause some distortion of the strong motion duration of the original record, an iterative process to correct the duration follows, if the error exceeds a predetermined tolerance. This process involves modification of the parts of the accelerogram that correspond to accumulation of 5% and 75% of Arias Intensity, such that the corresponding time interval equals the 5–75% significant duration of the original record. It should be noticed that the acceleration data points of the 10 greatest pulses remain intact, so that the matched IVs are not distorted. Again, care is

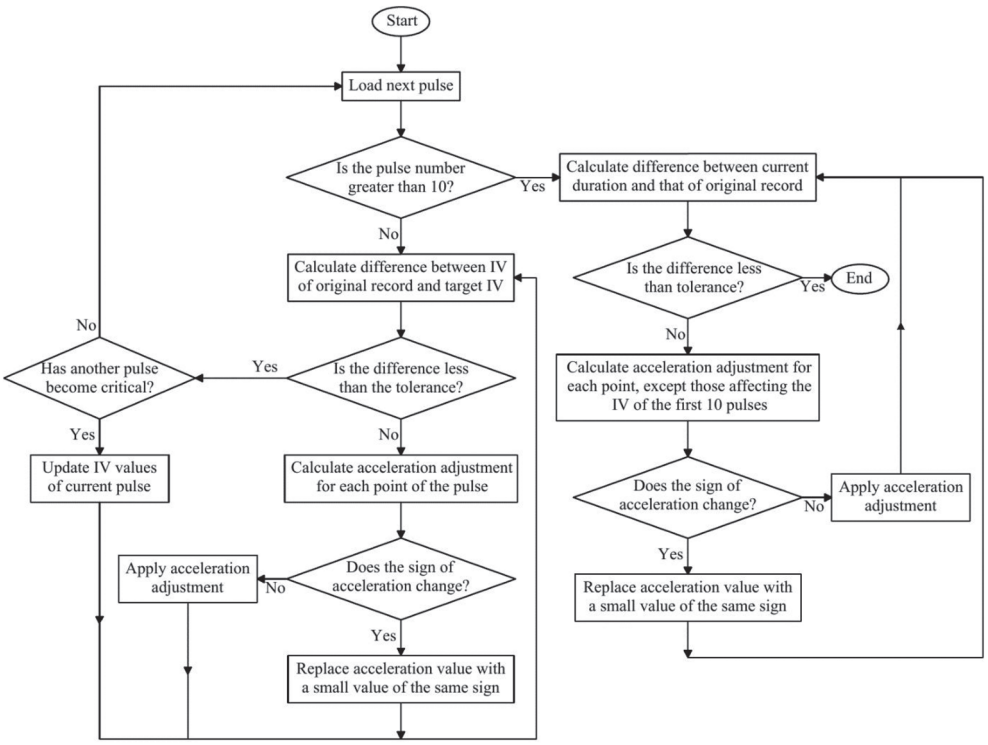

FIGURE 21 Flow chart of modification procedure

taken to avoid a change of sign of acceleration, because Arias Intensity is related to the square of acceleration and, hence, any change in acceleration is only meaningful if the sign is maintained. The algorithm terminates when the target error tolerance is attained.

The procedure described above ensures the generation of long records characterised by the same duration as those of the original dataset, as well as the target IV of the short-duration set. However, the spectral shape characteristics are not explicitly considered and may therefore be distorted as a result of the modification procedure. In order to ensure that no bias is introduced due to changes in spectral response of the modified long records, a subset of 65 records is selected from the original database of 101 long and 101 short ground motions. For these records, the acceleration response spectrum remains almost unchanged after the modifications required to achieve the target IV.

Hence, although the modification of the original records characteristics may be viewed as a limitation of the proposed methodology, it is expected that the differences due to the modification procedure are within acceptable limits, since the most significant ground motion characteristics (i.e., response spectrum and duration) are maintained. To illustrate this, the median response spectra of the long records before and after the modification are plotted in Figure 22, while Figure 23 shows the distribution of their 5–75% significant duration. It is noted that there are some slight differences in the distribution of duration between the original and modified records, as a tolerance of 5 s was employed to correct the duration of the latter.

The procedure proposed in this section should be viewed as a technique for considering the effect of pulses and not as an exhaustive methodology. It is limited to characterising the pulse distribution by means of IV and does not consider other parameters, such as the pulse duration, which has been shown to influence the structural response (e.g., Makris and Black[32]). Future studies could focus on improving this method by ensuring equivalence of pulses in terms of their duration or by adopting novel IMs, such as the recently proposed FIV3.[33] In addition, the first 10 pulses are employed herein, as suggested by Dávalos and Miranda.[25] Nevertheless, the number of pulses that influence mostly the response may also be further investigated.

7.3 | Comparative results

The SDOF models described in Section 2.1 are subjected to the 65 long records and their response spectrally equivalent short records, as well as the corresponding modified long seismic events, and the collapse capacities under each record set are then obtained through a series of IDAs. The main results are highlighted herein, focusing on the effect of duration on collapse. This is quantified by means of the percentage ratio of the difference in collapse capacity due to short

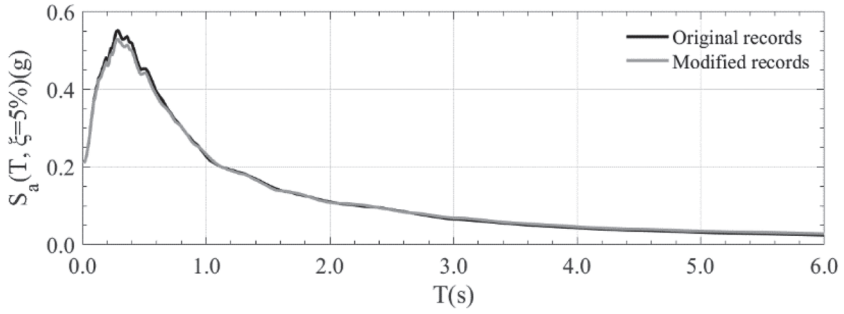

FIGURE 22 Geometric mean acceleration response spectra of original and modified long records

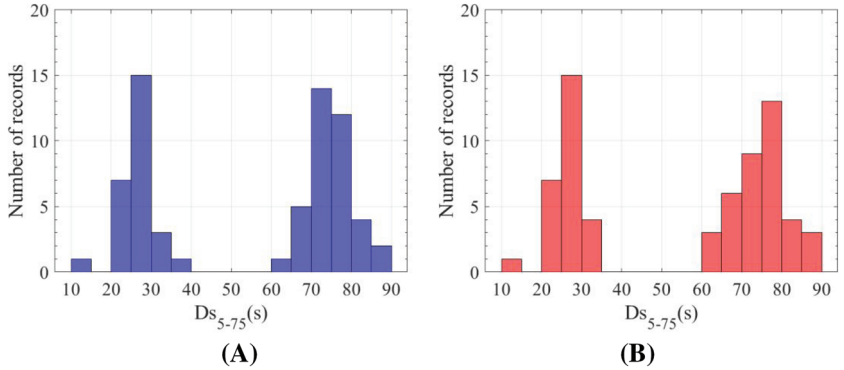

FIGURE 23 Distribution of 5–75% significant duration (Ds_{5-75}): original and B, modified long records [Colour figure can be viewed at wileyonlinelibrary.com]

and long records to the collapse capacity due to short records. Duration effects are evaluated using the modified set of long records, as well as the original long records. It is worth noting that the latter are not identical to the results presented in Section 4, because of the reduced size of the record datasets.

Figure 24 depicts the percentage reduction in collapse capacity for bilinear structural models characterised by fixed levels of ductility and strain hardening ($\mu_c = 4.0$ and $\alpha_h = 0.00$) and considering all possible combinations of period and level of P-Δ. The selected values of ductility and strain hardening are those for which duration effects are maximised, as discussed in Section 4. Similarly, Figure 25 refers to pinching systems with $\mu_c = 6.0$ and $\alpha_h = 0.10$.

It is evident that in the case of bilinear structural systems with $\mu_c = 4.0$ and $\alpha_h = 0.00$, almost no differences between the modified and original records are discerned. In contrast, the modification of the pulse content of long records influences the response of ductile hardening pinching systems. In particular, the maximum duration-induced decrease in collapse capacity amounts to almost 50% under the modified records as opposed to only 38% under the original long records for pinching hysteresis (Figure 25), while it remains around 55% in the case of bilinear hysteresis, which is similar to the reduction obtained without accounting for pulses (Figure 24). In order to highlight the differences between the original and modified record sets in the case of bilinear hysteresis, Figure 26 depicts duration effects in bilinear models with high ductility and strain hardening ratio ($\mu_c = 6.0$ and $\alpha_h = 0.10$). In this case, the decrease in collapse capacity due to duration, using the modified long records, reaches a maximum of 51%, which is significantly higher than the corresponding 38% when the original long set is employed.

The main effect of the modified set of records can therefore be observed in the case of long-period highly ductile systems (Figures 25 and 26). These systems exhibit some reduction in their collapse capacity when using long-duration records that are equivalent to the short records both in terms of response spectrum and pulses, compared with the case of using records that are equivalent only in terms of spectral response. Accordingly, duration effects appear to be more important. In fact, up to almost 23% (for $T = 3.0$ s, θ-$\alpha = 0.04$, $\mu_c = 6.0$, $\alpha_h = 0.10$ and bilinear hysteresis) more reduction in the collapse capacity of such systems is obtained due to duration when addressing the differences in pulses of short and long records. Hence, it can be concluded that apart from flexible ductile strain hardening models, the rest of the examined SDOFs do not show any significant change in their behaviour as a result of the influence of pulses, when IV is used as a metric to account for this effect. The reason why these models seem to be more affected by the pulse effect is attributed to their higher resistance to collapse. Since IV tends to increase with the ground motion scaling

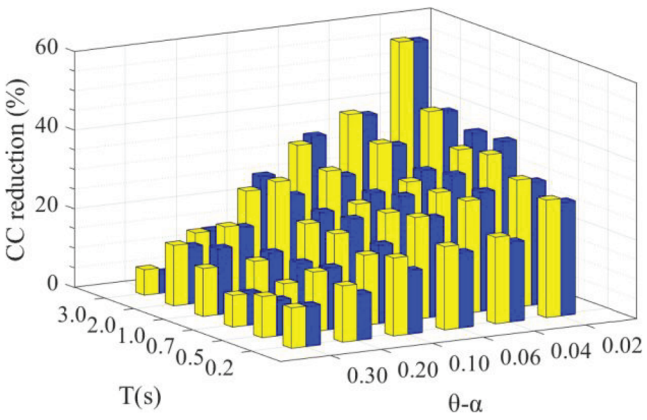

FIGURE 24 Collapse capacity reduction due to duration for bilinear systems with $\mu_c = 4.0$ and $\alpha_h = 0.00$ subjected to the original (blue colour) and the modified (yellow colour) sets of records [Colour figure can be viewed at wileyonlinelibrary.com]

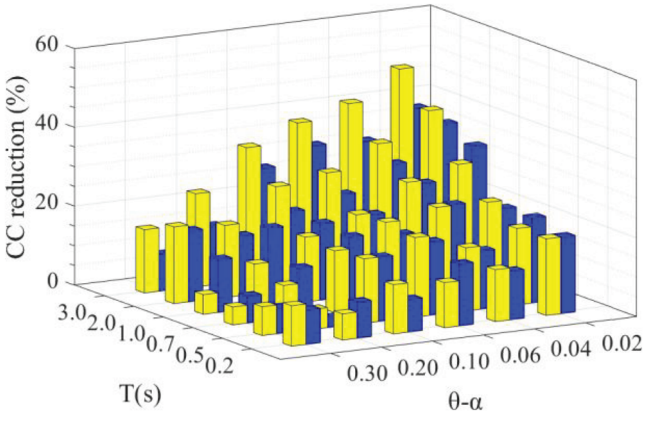

FIGURE 25 Collapse capacity reduction due to duration for pinching systems with $\mu_c = 6.0$ and $\alpha_h = 0.10$ subjected to the original (blue colour) and the modified (yellow colour) sets of records [Colour figure can be viewed at wileyonlinelibrary.com]

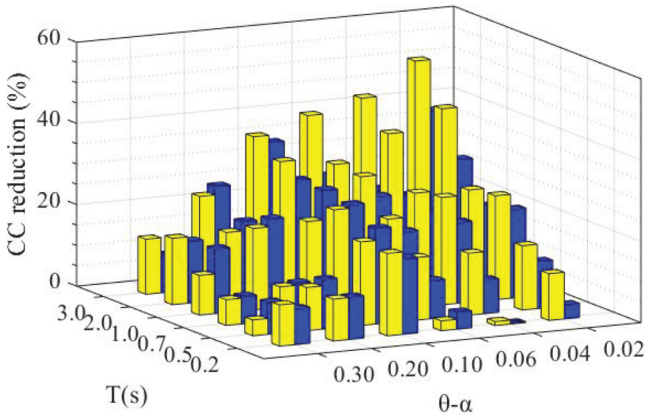

FIGURE 26 Collapse capacity reduction due to duration for bilinear systems with $\mu_c = 6.0$ and $\alpha_h = 0.10$ subjected to the original (blue colour) and the modified (yellow colour) sets of records [Colour figure can be viewed at wileyonlinelibrary.com]

factor, its effect is more significant at relatively high levels of intensity. Therefore, the higher the collapse capacity, the greater the effect of pulses is expected to be.

Based on the results presented in this section, it can be argued that accounting for the influence of acceleration pulses is crucial in order to achieve unbiased quantification of duration effects in some cases. In fact, even greater differences between the original and modified records could arise if accelerograms with different features in terms of pulses were used, as the results depend strongly on the pulse characteristics of the long and short seismic events.

8 | CONCLUDING REMARKS

This study has investigated the effect of strong motion duration on the collapse of ductile structural systems. For this purpose, response spectrally equivalent records were assembled and a series of ductile SDOF models characterised by different period, level of P-Δ, ductility, strain hardening ratio, and hysteretic behaviour were analysed. Through IDA, the collapse capacities of the examined models were evaluated, and the main trends of the response were identified. Although limited to SDOF oscillators, the current work provides useful insights into the collapse of structural systems. However, it is noted that future research should consider MDOF models to validate the applicability of the results obtained herein.

Similar to observations made in previous studies, the period of vibration and the strain hardening ratio were found to be beneficial to collapse resistance, while P-Δ effects were shown to be detrimental. Ductility enhances the collapse resistance, provided that the slope of the intermediate branch of the backbone curve remains positive after accounting for the P-Δ effects. Dispersion around the median collapse capacity was also quantified for long- and short-duration records, assuming a lognormal distribution. Lower levels of dispersion were obtained for long records compared with short ground motions, which is related to their lower collapse capacity, while increased record-to-record variability was obtained at high levels of period and low levels of P-Δ. Strong motion duration was found to play a key role in the collapse of ductile systems, being responsible for up to a 60% difference in collapse capacity, as observed in the case of flexible, bilinear systems subjected to low levels of P-Δ. The effects of duration depend primarily on the SDOF period, level of P-Δ and hysteretic behaviour, while the ductility and strain hardening ratio were shown to have a secondary role in comparison. Based on the collapse capacities of the SDOF models considered in this paper, duration-dependent collapse capacity spectra were developed, offering a simple and practical approach to account for duration effects when assessing the collapse capacity of ductile structures.

While collapse capacity was mostly employed throughout this work, comparison of the dispersion with that obtained using alternative IMs demonstrated its limitations, as also noted in other studies. IMs that account either for duration or acceleration pulses, quantified by means of maximum IV, were shown to perform better than those considering only the amplitude and spectral shape. Future collapse assessment investigations may consider such advanced intensity indexes, in order to achieve more stable estimates of the response with a lower number of earthquake records. Nevertheless, because of its simplicity and the availability of seismic hazard curves, spectral acceleration at the period of vibration is currently the most widely employed IM.

Finally, the effect of pulses was considered for the generation of pulse-modified equivalent long- and short-duration ground motion records in order to examine whether disregarding the influence of pulses could result in biased

estimations of strong motion duration effects. For this purpose, a novel method was developed in order to modify the long-duration set, such that each long record has the same spectral shape and IV characteristics as its short counterpart. The IVs of the 10 largest pulses were employed, which are believed to influence mostly the response. However, it should be noted that the specific number of pulses needs to be determined within further sensitivity assessments. In addition, future research could incorporate the duration of pulses in the modification procedure, which has been shown by previous studies to influence significantly the damage potential of ground motion records. The SDOF models under investigation were subjected to both the original and modified set of long records, in addition to the set of short earthquakes. The effect of duration, as obtained using the original and modified sets, was found to differ most significantly in the case of flexible ductile systems, with the differences reaching up to 23% for bilinear models. These results suggest that acceleration pulses need to be incorporated when estimating the collapse capacity, particularly for long-period ductile structures.

ACKNOWLEDGEMENTS

The first author would like to acknowledge the support provided by the Skempton Scholarship from Imperial College London and by the scholarship from Onassis Foundation in Greece.

ORCID

Miguel A. Bravo-Haro https://orcid.org/0000-0003-0757-777X
Ahmed Y. Elghazouli https://orcid.org/0000-0002-0038-7415

REFERENCES

1. Haselton CB, Liel AB, Deierlein GG. Simulating structural collapse due to earthquakes: model idealization, model calibration, and numerical solution algorithms. In *Proc. 2nd International Conference on Computational Methods in Structural Dynamics and Earthquake Engineering (COMPDYN 2009)* (Papadrakakis M, Lagaros ND, Fragiadakis M. eds). June 22–24, 2009, Rhodes, Greece, CD-ROM, paper no. CD497 (2009).
2. Miranda E, Akkar SD. Dynamic instability of simple structural systems. *J Struct Eng*. 2003;129:1722-1726.
3. Adam C, Jäger C. Seismic collapse capacity of basic inelastic structures vulnerable to the P-delta effect. *Earthquake Eng Struct Dynamics*. 2012;41:775-793.
4. Tsantaki S, Wurzer L, Jäger C, Adam C, Oberguggenberger M. Refined analytical collapse capacity spectra. *Iranian J SciTechnol Trans Civil Eng*. 2015;39:253-270.
5. Vamvatsikos, D, Akkar, SD and Miranda, E. Strength reduction factors for the dynamic instability of oscillators with nontrivial backbones. Conference on Computational Methods in Structural Dynamics and Earthquake Engineering, 2009.
6. Han SW, Moon KH, Chopra AK. Application of MPA to estimate probability of collapse of structures. *Earthquake Eng Struct Dynamics*. 2010;39:1259-1278.
7. Foschaar, J, Baker, J and Deierlein, G. Preliminary assessment of ground motion duration effects on structural collapse. Proceedings of the 15th World Conference on Earthquake Engineering, 2012.
8. FEMA. *Quantification of Building Seismic Performance Factors*. US Department of Homeland Security, Washington DC, FEMA; 2009.
9. Trifunac MD, Brady AG. A study on the duration of strong earthquake ground motion. *Bull Seismol Soc Am*. 1975;65:581-626.
10. Raghunandan M, Liel AB. Effect of ground motion duration on earthquake-induced structural collapse. *Struct Safety*. 2013;41:119-133.
11. Raghunandan M, Liel AB, Luco N. Collapse risk of buildings in the Pacific northwest region due to subduction earthquakes. *Earthq Spectra*. 2015;31:2087-2115.
12. Chandramohan R, Baker JW, Deierlein GG. Quantifying the influence of ground motion duration on structural collapse capacity using spectrally equivalent records. *Earthq Spectra*. 2016;32:927-950.
13. Somerville PG, Smith NF, Graves RW, Abrahamson NA. Modification of empirical strong ground motion attenuation relations to include the amplitude and duration effects of rupture directivity. *Seismol Res Lett*. 1997;68:199-222.
14. Bravo-Haro MA, Elghazouli AY. Influence of earthquake duration on the response of steel moment frames. *Soil Dynamics Earthquake Eng*. 2018;115:634-651.
15. Bravo-Haro, MA, Liapopoulou, M and Elghazouli, AY. Seismic collapse capacity assessment of SDOF systems incorporating duration and instability effects. *Bull Earthquake Eng*. 2020. https://doi.org/10.1007/s10518-020-00829-9
16. Kostinakis K, Fontara I-K, Athanatopoulou AM. Scalar structure-specific ground motion intensity measures for assessing the seismic performance of structures: a review. *J Earthquake Eng*. 2018;22:630-665.
17. Marafi NA, Berman JW, Eberhard MO. Ductility-dependent intensity measure that accounts for ground-motion spectral shape and duration. *Earthquake Eng Struct Dynamics*. 2016;45:653-672.
18. Cordova, PP, Deierlein, GG, Mehanny, SS and Cornell, CA. Development of a two-parameter seismic intensity measure and probabilistic assessment procedure. The Second US-Japan Workshop on Performance-Based Earthquake Engineering Methodology for Reinforced Concrete Building Structures, 2000. 187–206.

19. Luco N, Cornell CA. Structure-specific scalar intensity measures for near-source and ordinary earthquake ground motions. *Earthq Spectra*. 2007;23:357-392.
20. Bianchini, M, Diotallevi, P and Baker, J. Prediction of inelastic structural response using an average of spectral accelerations. 10th International Conference on Structural Safety and Reliability (ICOSSAR09), 2009.
21. Bojórquez E, Iervolino I. Spectral shape proxies and nonlinear structural response. *Soil Dynamics Earthquake Eng*. 2011;31:996-1008.
22. Eads L, Miranda E, Lignos DG. Average spectral acceleration as an intensity measure for collapse risk assessment. *Earthquake Eng Struct Dynamics*. 2015;44:2057-2073.
23. Tsantaki, S, Jäger, C and Adam, C. Improved seismic collapse prediction of inelastic simple systems vulnerable to the P-delta effect based on average spectral acceleration. Proceedings of the 15th World Conference on Earthquake Engineering (15 WCEE), 2012.
24. Bertero VV, Mahin SA, Herrera RA. Aseismic design implications of near-fault San Fernando earthquake records. *Earthquake Eng Struct Dynamics*. 1978;6:31-42.
25. Dávalos H, Miranda E. Evaluation of bias on the probability of collapse from amplitude scaling using spectral-shape-matched records. *Earthquake Eng Struct Dynamics*. 2019;48:970-986.
26. Jayaram N, Lin T, Baker JW. A computationally efficient ground-motion selection algorithm for matching a target response spectrum mean and variance. *Earthq Spectra*. 2011;27:797-815.
27. Ibarra LF, Krawinkler H. *Global Collapse of Frame Structures Under Seismic Excitations*. Berkeley, CA: Pacific Earthquake Engineering Research Center; 2005.
28. McKenna, F, Mazzoni, S and Fenves, G. 2011. Open system for earthquake engineering simulation (OpenSees) software version 2.2. 0. University of California, Berkeley, CA. Available from http://opensees.berkeley.edu.
29. Vamvatsikos D, Cornell CA. Incremental dynamic analysis. *Earthquake Eng Struct Dynamics*. 2002;31:491-514.
30. Rahnama M, Krawinkler H. In: John A, ed. *Effects of Soft Soil and Hysteresis Model on Seismic Demands*. Standford, CA: Blume Earthquake Engineering Center; 1993.
31. Kohrangi M, Vamvatsikos D, Bazzurro P. Pulse-like versus non-pulse-like ground motion records: spectral shape comparisons and record selection strategies. *Earthquake Eng Struct Dynamics*. 2019;48:46-64.
32. Makris N, Black CJ. Dimensional analysis of bilinear oscillators under pulse-type excitations. *J Eng Mech*. 2004;130:1019-1031.
33. Dávalos H, Miranda E. Filtered incremental velocity: a novel approach in intensity measures for seismic collapse estimation. *Earthquake Eng Struct Dynamics*. 2019;48:1384-1405.

How to cite this article: Liapopoulou M, Bravo-Haro MA, Elghazouli AY. The role of ground motion duration and pulse effects in the collapse of ductile systems. *Earthquake Engng Struct Dyn*. 2020;1–21. https://doi.org/10.1002/eqe.3278